Nanoscale Advances

PAPER

View Article Online
View Journal | View Issue

Cite this: *Nanoscale Adv.*, 2020, **2**, 5403

White-light-emitting triphasic fibers as a phosphor for light-emitting diodes†

Weidong Han,[a] Su-Hyeong Chae,[a] Taewoo Kim,[a] Daewoo Lee[b] and Hakyong Kim *[ab]

White-light-emitting materials have received significant attention because of their potential application in lighting, displays, and sensors. However, it is a challenge to obtain white light from one phosphor, because the basic requirement of the white light emission spectrum is that it should be wide enough to cover the entire visible light region. In this study, we have designed and demonstrated a white-light-emitting PMMA–CBS-127/PVP–coumarin 6/PAN–rhodamine B (PSCR) fibrous membrane, which was prepared through a triphasic electrospinning method. Three luminescent organic dyes, CBS-127 (4.77 wt%, blue), coumarin 6 (0.1 wt%, green), and rhodamine B (0.42 wt%, red), were elaborately selected and doped into PMMA, PVP, and PAN, respectively. The resulting flexible PSCR membranes show white light emission (cover the entire visible-light region from 382 to 700 nm) with Commission Internationale de L'Eclairage (CIE) coordinates of (0.31, 0.32), which is very close to ideal white light with CIE coordinates (0.33, 0.33). In addition, the PSCR membranes maintained high-quality white light emission after about 10 weeks of storage. The PSCR membranes can be used as the phosphor converting layer in white light-emitting diodes (WLEDs) through a remote membrane packaging method. A bright white emission is achieved at an applied voltage of 9 V. Therefore, the results indicate that PSCR membranes are potentially attractive candidates for application in WLEDs and displays.

Received 16th May 2020
Accepted 22nd September 2020

DOI: 10.1039/d0na00396d

rsc.li/nanoscale-advances

1. Introduction

In recent years, white-light-emitting materials have received significant attention because of their potential application in light emitting diodes (LEDs),[1] backlight for displays,[2] and sensors.[3] Up until now, a large number of white-light-emitting materials have been studied extensively, such as organic dyes,[4] inorganic phosphors,[5] polymers,[6] quantum dots,[7] perovskites,[8,9] interconnected boron nitride hollow microtubes,[10] and metal–organic frameworks.[11] However, it remains challenging to obtain a high-quality white-light emission from one phosphor. The white emission spectrum should be wide enough to cover the entire visible area and close to the Commission Internationale de L'Eclairage (CIE) coordinates (0.33, 0.33).

In various white-light-emitting materials, white light is obtained from using a mixture of three primary fluorescent dyes, emitting red, green, and blue light. However, when the distance between the mixed fluorescent dyes is less than 10 nm, mixing fluorescent dyes usually result in fluorescence resonance energy transfer (FRET) from short-wavelength emission to long-wavelength emission. The FRET efficiency can reach 90% and even cause fluorescence quenching to occur due to interactions between fluorescent dyes.[12,13] Because the FRET from the donor to the acceptor is too strong, a wider emission band is obtained in the visible spectral range and its efficiency is reduced. There are still huge challenges in solving the above problems. Therefore, it is strongly recommended to use a matrix material to isolate each fluorescent dye to solve the FRET problem so that the interaction between the donor and acceptor dyes is negligible. In order to achieve effective dye separation, it has been reported that different dye molecules can be encapsulated into host materials to control the relative distance the donor and acceptor or the surrounding environment can be adjusted to achieve the inhibition of energy transfer between different fluorescent molecules.[14,15]

Electrospinning is a simple, fast, and promising technology for preparing fibrous materials with a high porosity structure and diameters both on the micro- and nano-scales. Electrospun nanofibers have been broadly studied and various functional nanofibers were obtained, such as inorganic,[16] organic polymers,[17,18] biomacromolecules,[19] and composite materials.[20] In recent years, the electrospinning approach has emerged as a viable option for a variety of optoelectronic devices and applications. In the past decade, various electrospun fluorescent fibers have been developed by incorporating fluorescent dyes.[21–23] The fabrication of dye-doped active electrospun nanofibers has motivated extensive studies on optoelectronic

[a]*Department of BIN Convergence Technology, Jeonbuk National University, Jeonju 54896, South Korea. E-mail: khy@jbnu.ac.kr*

[b]*Department of Organic Materials & Fiber Engineering, Jeonbuk National University, Jeonju 54896, South Korea*

† Electronic supplementary information (ESI) available. See DOI: 10.1039/d0na00396d

applications involving lasers,[24] light-emitting sources,[25] and optical sensors.[26] Pan and co-workers showed that a white light-emitting nanofiber with a core–shell structure was prepared using coaxial electrospinning technology. The core–shell structure can spatially isolate donor and acceptor dyes to avoid FRET between them. However, the outer polymer of the shell structure has a blocking effect, resulting in a decrease in the emission efficiency of white light.[27] Triphasic nanofibers were fabricated through multi-nozzle electrospinning equipped with three parallel jetting capillaries. By constructing triphasic nanofibers, three different dopants can separate into different sides of a single fiber. This triphasic structure can significantly reduce the interface between additives in different phases inside the fiber, so that different sides play different functions.[28] This method would provide a unique way to make white fluorescent nanofibers.

In this work, we fabricated a flexible uniform white-light-emitting PMMA–CBS-127/PVP–coumarin 6/PAN–rhodamine B (PSCR) fibrous membrane by a triphasic electrospinning method. A multi-nozzle electrospinning equipment enables the separation of CBS-127 (blue), coumarin 6 (green), and rhodamine B (red) dyes in different polymer matrices, which can well inhibit the FRET between the dyes. Besides, we also show the application of the fibrous membrane in combination with commercial UV light emitting diodes (LED) to obtain white light emission.

2. Experimental section

2.1 Materials

CBS-127 (S), coumarin 6 (C), and rhodamine B (R) were purchased from Aladdin Reagent Co., Ltd., China (Fig. S1†). *N*,*N*-Dimethylformamide (DMF, anhydrous, 99.8%) was purchased from Samchun Pure Chemical Co., Ltd., South Korea. Polyvinylpyrrolidone (PVP) (M_w = 1 300 000), polyacrylonitrile (PVP) (M_w = 150 000), and poly(methyl methacrylate) (PMMA) (M_w = 350 000) were obtained from Sigma Aldrich Co., Ltd., South Korea. The LED chips (365 nm) were provided by Kiwi Lighting Company, China.

2.2 Synthesis of PMMA–S, PVP–C, and PAN–R fibrous membranes

Firstly, three fibers were synthesized by single nozzle electrospinning. PMMA–S:PMMA (12 wt%) was dissolved in DMF. After stirring for 12 h at 50 °C, CBS-127 (4.77 wt%) was added to the PMMA solution with continuous stirring for 12 h; PAN–R:PAN (8 wt%) was dissolved in DMF. After stirring for 12 h at 50 °C, rhodamine B (0.8 wt%) was added to the PAN solution with continuous stirring for 12 h; PVP–C:PVP (15 wt%) was dissolved in DMF. After stirring for 12 h at room temperature, coumarin 6 (1.8 wt%) was added to the PVP solution with continuous stirring for 12 h. All the solutions were gently stirred until getting a uniform polymer solution. The electrospinning was performed on an in-house developed single-nozzle electrospinning machine at a high voltage of 18 kV. The nozzle was located at a distance of 15 cm from the cylinder's collector wrapped with slick paper. The temperature and humidity of the electrospinning process were controlled at 25 ± 5 °C and 45% ± 5%, respectively. Fibrous membranes were obtained and were named PMMA–S, PVP–C, and PAN–R, respectively. For comparative purposes, PAN–S/C/R (S (4.77 wt%)/C (1.8 wt%)/R (0.8 wt%)) fibrous membranes were prepared by single nozzle electrospinning. PAN–S/C/R:PAN (8 wt%) was dissolved in DMF *via* stirring for 12 h at 50 °C. Then, CBS-127 (4.77 wt%), coumarin 6 (1.8 wt%), and rhodamine B (0.8 wt%) were added to the PAN solution with continuous stirring for 12 h. Subsequently, a PAN–S/C/R membrane was fabricated by the same procedure as mentioned above.

2.3 Synthesis of PSCR fibrous membranes

Base on the above conditions for preparing the PMMA–S, PVP–C, PAN–R fibrous membranes, PMMA–S, PVP–C, and PAN–R solutions were prepared by adding different amounts of dye to the polymer solution (4.77 wt% S, 0.1 wt% C, and 0.42 wt% R, respectively). The above solutions were poured in three plastic syringes, respectively. Then, the three syringes were connected to a three-channel parallel electrospinning nozzle through a pipeline to prepare the fibers (Fig. S2†). The structure of the triple side-by-side spinneret is illustrated in Fig. S3.† The device consists of four parts: spinneret, sealing block, PTFE shell, and fixing screw. The stainless spinneret consists of three capillary channels (inner diameter (ID) of 0.6 mm) in Fig. S3a and c.† Three channels are used for delivering the different polymer solutions, which are combined in a plastic channel that forms the outlet (inner diameter (ID) of 0.5 mm, length 30 mm) (Fig. S2d†). Subsequently, the three plastic syringes were fixed to one pump (Fusion 200, Chemyx Inc., USA). The PMMA–S, PVP–C, and PAN–R solutions were pumped at feed rates of 0.1 μl min^{-1}. The plastic nozzle was located at a distance of 15 cm from the cylinder's collector wrapped with slick paper. The fixing screw can be connected to the high-voltage power supply through a copper wire. The applied voltage was kept at 18 kV. The temperature and humidity of the electrospinning process were controlled at 25 ± 5 °C and 45% ± 5%, respectively. For comparative purposes, PMMA/PVP/PAN fibrous membranes without fluorescent dyes were prepared by the same procedure as mentioned above.

2.4 Fabrication of WLEDs

In order to make practical devices, the PSCR fibrous membrane was cut to a size of 1 × 1 cm^2 area. The thickness of the membrane was ~45 μm recorded using a thickness tester. A GaN-based ultraviolet-emitting LED (UV LED) was attached on a heat sink and there was no overcoat material above the chips (45 × 45 mil, 3 pieces). The peak wavelength of the UV LED chips was 365 nm, and the operating current was 350 mA. The two leads on the LED were prepared to connect to the power supply. Then, the PSCR membrane was placed on the top of the LED chips by a convenient remote packaging method.

2.5 Characterization

Scanning electron microscope (SEM) images were obtained on a Hitachi S-4700 scanning electron microscope. The photoluminescence spectra were collected using a PerkinElmer LS-55 fluorescence spectrometer with xenon discharge lamp

excitation. UV-Vis absorption measurements were performed using a UV-2600 Spectrophotometer equipped with deuterium and tungsten halide as light sources (SHIMADZU Instruments). The tensile mechanical properties of samples were obtained by using a LR5K Plus tensile tester (LLOYD Instruments). The testing samples were prepared in the form of standard dumb-bell shapes according to ASTM standard D882-10. The thicknesses of the samples were measured using a digital micrometer (Mitutoyo Digimatic Thickness Gauge ID-C1012BS) with a precision of 1 μm. Testing was done at a crosshead speed of 5 mm min^{-1}. Five specimens were used for sample, and the tensile strength was calculated based on the engineering stress–strain curve obtained from the instrument data, the average of which was used as the tensile strength of the sample. The optical properties of the white LED were measured by using a HAAS-2000 high accuracy array spectroradiometer with an integrating sphere (Everfine Photo-E-Info Co., LTD). All the measurements were performed at room temperature.

3. Results and discussion

The preparation of hybrid multicompartmental PSCR fibrous membranes is schematically illustrated in Fig. 1. In our research, the laminar flow of three distinct polymer solutions is pumped through a modified nozzle with a tri-channel spinneret at a feed rate of −0.1 μl min^{-1} (Fig. S2 and S3†). With the

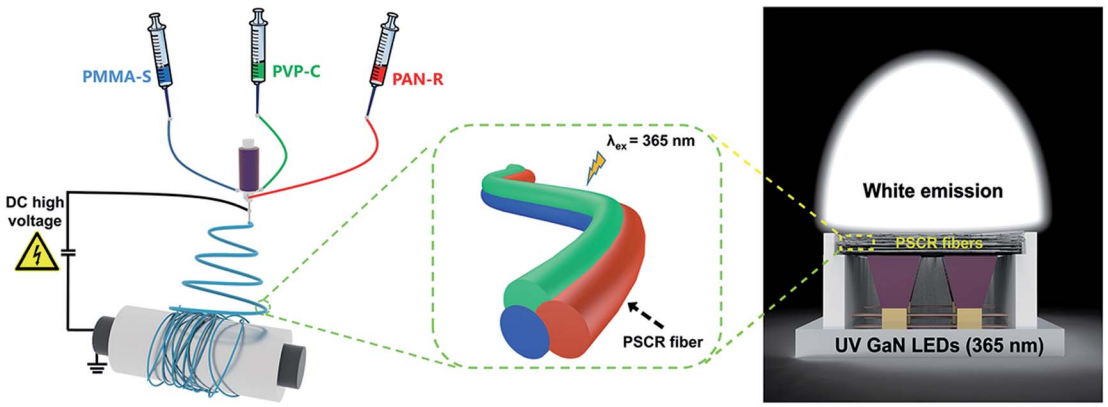

Fig. 1 Schematic illustration of the fabrication of PSCR fibers by a triphasic electrospinning method.

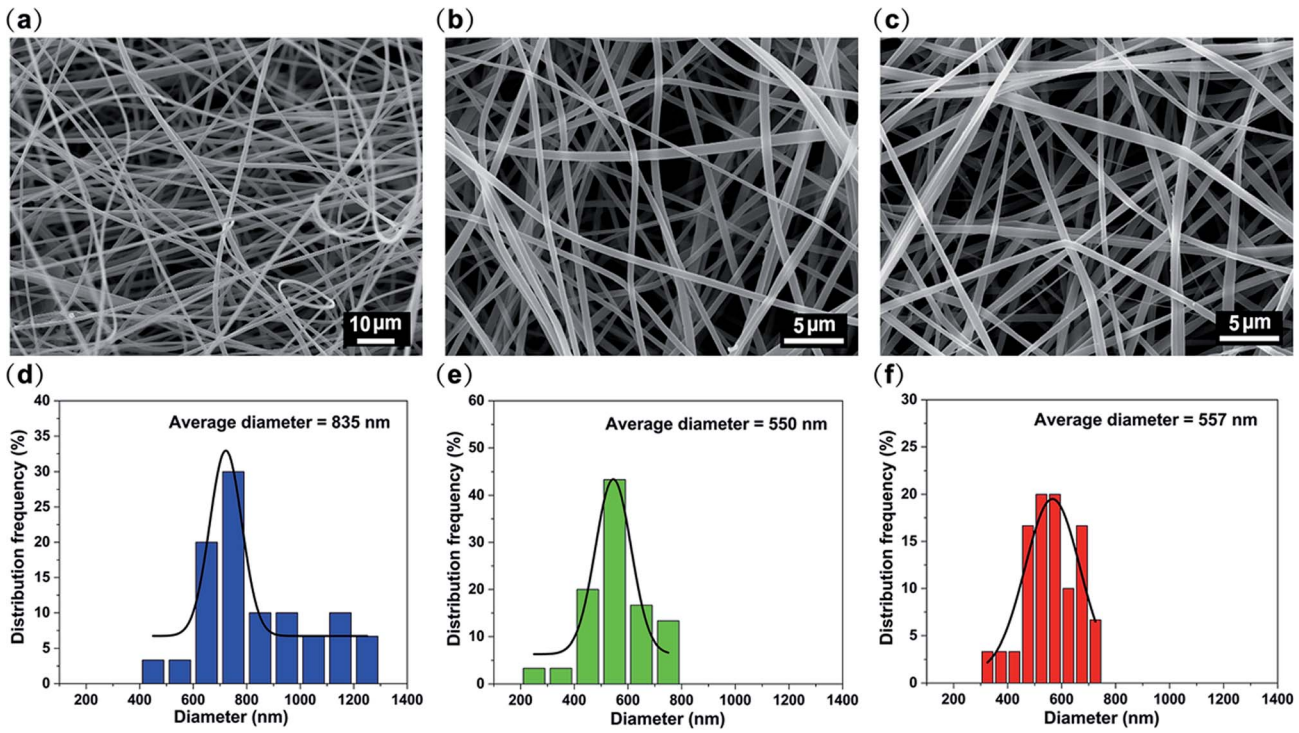

Fig. 2 SEM image of (a) PMMA–S, (b) PVP–C, and (c) PAN–R fibrous membranes. The diameter distribution of (d) PMMA–S, (e) PVP–C, and (f) PAN–R fibrous membranes.

different spinning solutions into the three channels of the spinneret, the distribution of components within the fiber is consistent with that within the spinning spinneret channel after fiber formation. Through the triphasic spinneret, the triphasic polymer/polymer interface was maintained between the three jetting fluids throughout the nozzle until electrified jetting occurred. The physical space isolation of the fluorescent dyes can be easily achieved through the triphasic electrospinning approach, while suppressing the occurrence of FRET between different dyes and achieving a wide range of the visible spectrum.

3.1 PMMA–S, PVP–C, and PAN–R fibrous membranes

To choose a right red, green and blue primary color fluorescent dye among the diverse fluorescent dyes, we firstly try CBS-127, coumarin 6, and rhodamine B as combined emitters. PMMA–S, PVP–C, and PAN–R fibrous membranes were fabricated through single-nozzle electrospinning, respectively. The morphologies of the three kinds of nanofibers were evaluated by SEM. Fig. 2a–c exhibit the SEM images of PMMA–S, PVP–C, and PAN–R nanofibers, with an average diameter of 835, 550, and 557 nm (Fig. 2d–f), respectively. Under the optimized conditions, the nanofibers were smooth and homogeneous in all groups. Fig. 3a–c show the photoluminescence (PL) spectra of PMMA–S, PVP–C, and PAN–R fibrous membranes, which show an emission peak at 431 nm, 531 nm, and 608 nm with a corresponding excitation peak at 365 nm. Digital photographs of the PMMA–S, PVP–C, and PAN–R membranes with a tailored size of 3 × 7 cm in the natural state are shown in Fig. 3d (up). The optical image of the PMMM-S (blue), PVP-C (green), and PAN-R (red) fibrous membranes were excited using UV light (365 nm), as illustrated in Fig. 3d (down). Moreover, as shown in the CIE chromaticity coordinates (Fig. 3e), the CIE coordinates for the PMMA–S, PVP–C, and PAN–R fibrous membranes were calculated to be (0.15, 0.05), (0.3, 0.65), and (0.61, 0.35), respectively. Through a simple doping process, we have achieved composite fibrous membranes emitting blue, green, and red light, respectively. Therefore, it is possible to assemble three kinds of nanofibers to achieve a fibrous membrane for white light emission. As predicted, the white-light emission was

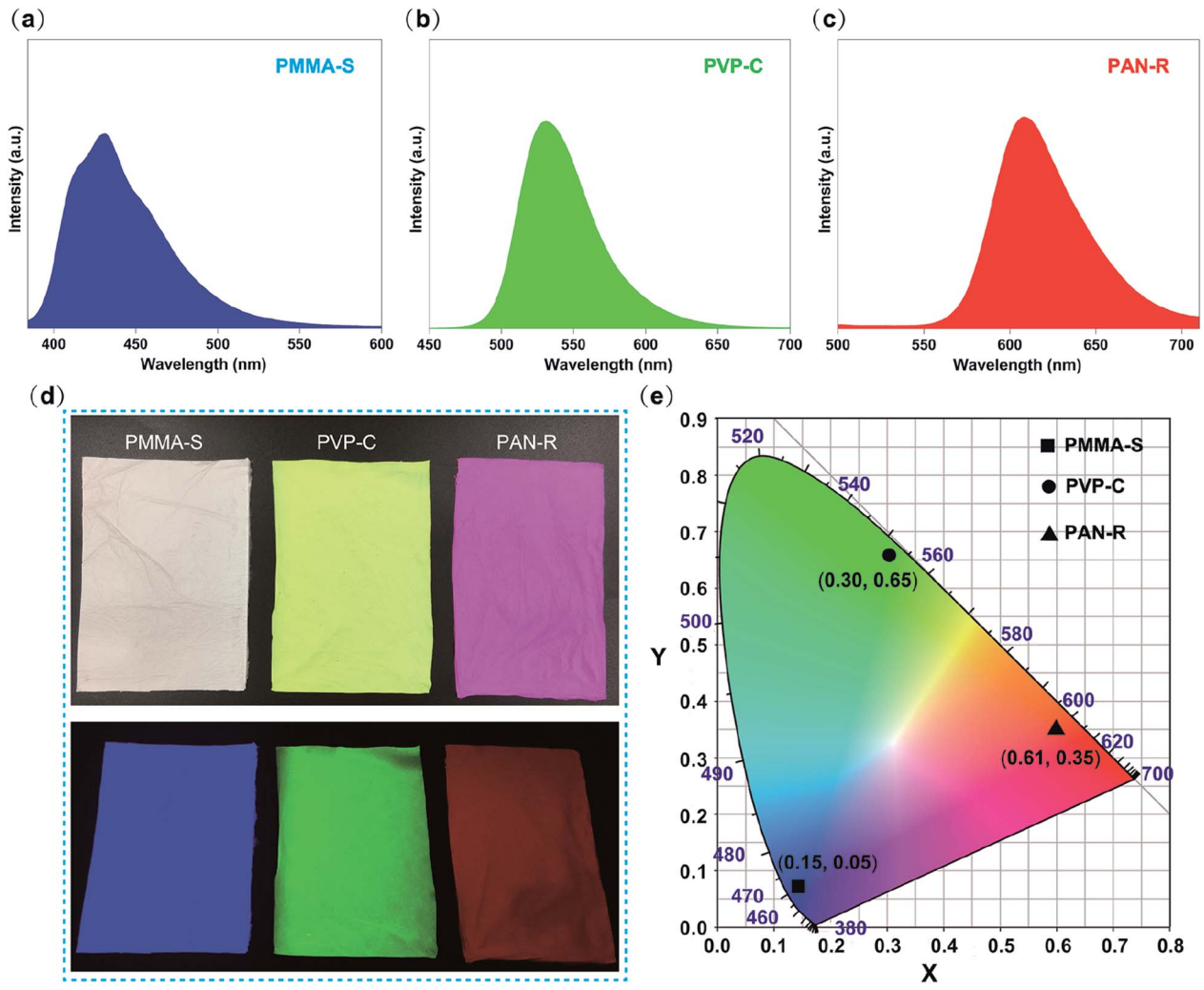

Fig. 3 PL spectrum of (a) PMMA–S, (b) PVP–C, and (c) PAN–R fibrous membranes. (d) Photograph of PMMA–S, PVP–C, and PAN–R membranes under white light (up) and a UV lamp (365 nm) (down). (e) CIE chromaticity diagram of PMMA–S, PVP–C, and PAN–R fibrous membranes.

achieved by optimizing the ratio of PMMA–S, PVP–C, and PAN–R fibers.

3.2 PSCR fibrous membranes

White light can be considered as a balanced composition of three basic lights: red, green, and blue. Although it seems easy, the generation of white light in luminescent materials is a very difficult job.[29–33] The above results have proven that PMMA–S, PVP–C, and PAN–R fibers have blue, green and red luminous properties, respectively. Therefore, if the S, C and R content ratios contained in PMMA, PVP, and PAN are properly adjusted, white light can be achieved by balancing their luminescence. Encouragingly, white light PSCR fibers were obtained by combining three dye materials under optimized conditions. Three parallel capillary channels were designed in the home-made electrospinning nozzle device (Fig. S3†). The three spinning solutions extend through the needle to the outlet of the plastic nozzle area in a laminar state. Due to the differences between the three spinning solutions, three completely different interfaces can be formed in the plastic nozzle area.[34,35] During the electrospinning process, the three spinning solutions at the tip of the plastic nozzle will form a parallel structure due to the differences in the properties of different polymers, and then they will form a triphasic Tylor cone and a triphasic jet by the electric field force. The triphasic jet is continuously stretched and drawn into a fibrous shape, and solidified with the continuous evaporation of the solvent, and finally a triphasic fiber is obtained.

The morphologies of the PSCR fibers were examined by using SEM (Fig. 4a and b). Numerous randomly distributed fibers with an average diameter of 1063 nm through a triphasic electrospinning process were obtained (Fig. 4c). The fibers are confirmed to be smooth, relatively uniform in diameter and continuous. The typical stress–strain curve of the PSCR membrane is shown in Fig. 4d. It can be seen that the PSCR membrane displays a linear elastic behavior with continuously applied stress until the fibers break. The tensile strength of the PSCR membrane is 1.89 MPa. The above results suggest that the PSCR membrane possesses appropriate mechanical properties and could be applied as a promising material for LEDs. The emission spectrum of the PSCR membrane covers the most of the visible spectrum region (ranging from 382 to 700 nm) (Fig. 5a). The CIE chromaticity coordinates of the PSCR membrane are (0.31, 0.32) (Fig. 5b), which are very close to those

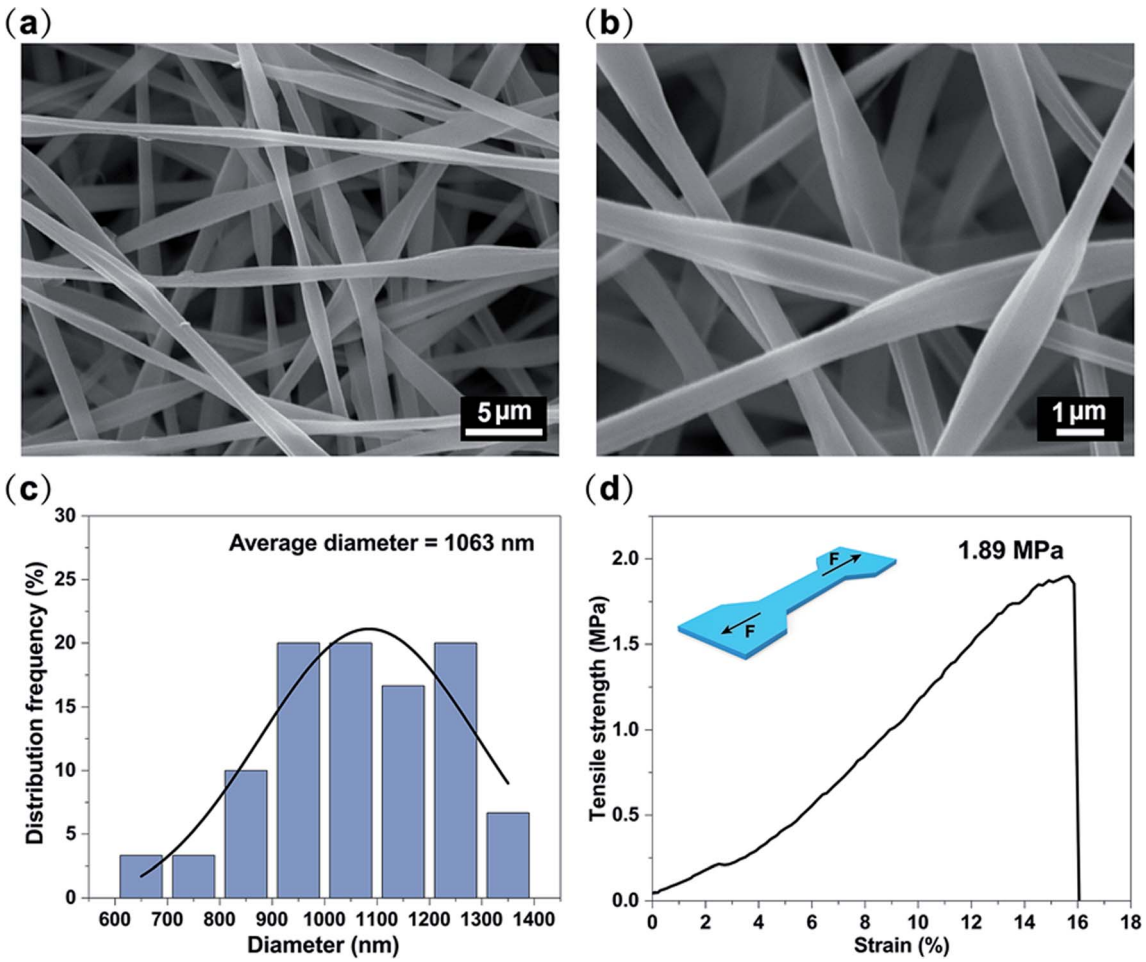

Fig. 4 (a and b) SEM image of PSCR fibrous membranes. (c) The diameter distribution of PSCR fibrous membranes. (d) Stress–strain curve of the PSCR fibrous membranes.

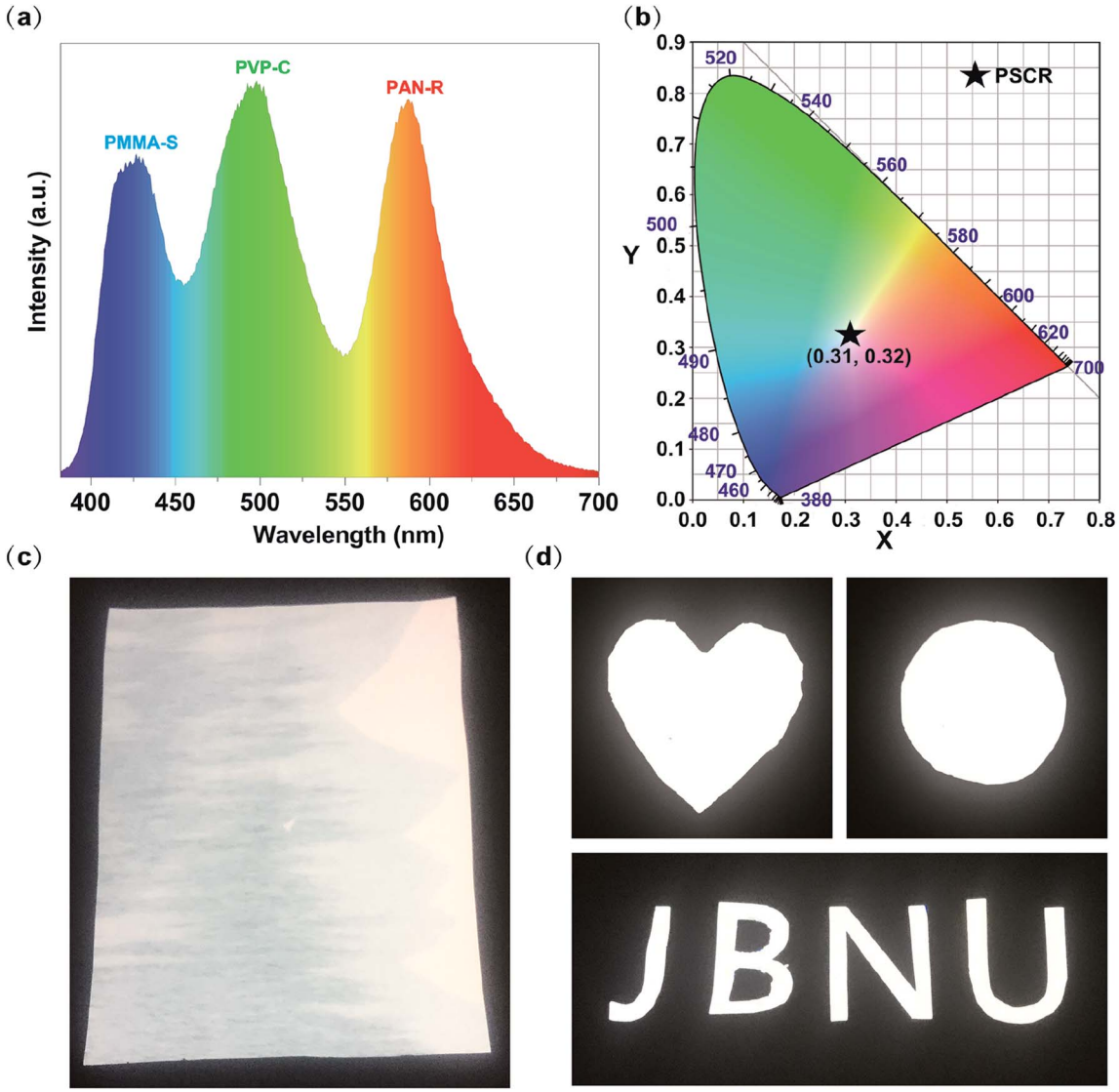

Fig. 5 (a) PL spectrum of the PSCR fibrous membrane. (b) CIE chromaticity diagram of the PSCR fibrous membrane. (c) Photograph of the PSCR fibrous membrane under a UV lamp (365 nm). (d) Different shapes of the PSCR fibrous membranes after being cropped.

(0.33, 0.33) of the ideal white light emitting materials. A white light emission PSCR membrane can be realized together with UV light for excitation (365 nm) (Fig. 5c). In addition, the operability of the PSCR membrane is demonstrated in Fig. 5d; the resulting membrane can be cut into any shape desired, such as a heart, circle, or even the letters of "J", "B", "N", and "U". All investigated scaffolds showed that the triphasic electrospinning method can be applied as a strategy to achieve white light.

Meanwhile, we have compared the PSCR membrane prepared by triphasic electrospinning to the PAN–S/C/R membrane prepared by single-nozzle electrospinning. The SEM images of the PAN–S/C/R membrane are shown in Fig. S4a.† The fibers were smooth and homogeneous. The optical image of the PAN–S/C/R membrane was excited using UV light (365 nm), and the formed membrane emits red fluorescence, as illustrated in Fig. S4b.† Moreover, as shown in the CIE chromaticity coordinates (Fig. S4c†), the CIE coordinates for the PAN–S/C/R membrane were calculated to be (0.51, 0.30), and it could be seen that the coordinates reach the red region.

Fig. S5a† shows the PL spectra of PAN–S/C/R and PSCR membranes. The emission of the PAN–S/C/R membrane at 595 nm was dramatically enhanced, whereas the emission of the membrane at 430 nm and 498 nm was significantly decreased, compared to that of the PSCR membrane. These results indicate that the direction of FRET occurred from S to C and then from C to R because the energy is transferred step-by-step from a high-energy to a low-energy state (Fig. S5c†). Thus, when three different fluorescent dyes suitable for FRET were concurrently loaded into a PAN–S/C/R fiber (Fig. S4 and S5†), red emission from the fiber was generated because the three dyes were located within the Förster radius (Fig. S5c†). In contrast, white emission was created when the three dyes were isolated in independent polymer matrices (PMMA–S/PVP–C/PAN–R) (Fig. S5b†), which can significantly reduce the FRET

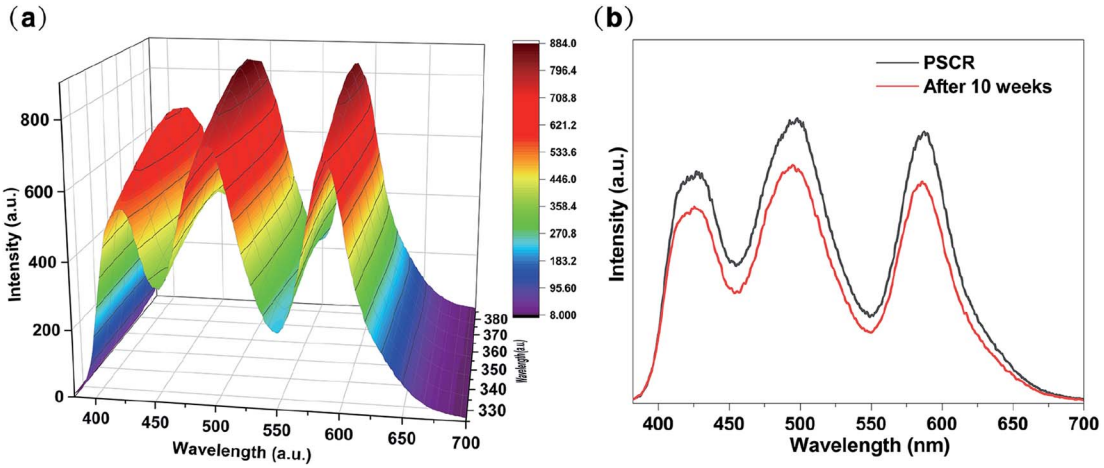

Fig. 6 (a) PL spectrum of the PSCR fibrous membrane with excitation wavelengths varied from 325 to 385 nm. (b) Comparison of the PL spectra of PSCR fibrous membranes (fresh *vs.* after 10 weeks).

caused by the aggregation of dye molecules.[36–39] It can be attributed to the separation of dye molecules inside the polymer suppressing their intramolecular torsional motion.[40,41]

Likewise, to evaluate the stability of PSCR fibrous membranes, when the excitation wavelength is changed from 325 nm to 385 nm, the PSCR membrane always emits white light. When the excitation wavelength is greatly changed, there is only a small change in white light emission (Fig. 6a and S7†). In addition, the obtained PSCR membranes maintained high-quality white light emission after about 10 weeks of storage

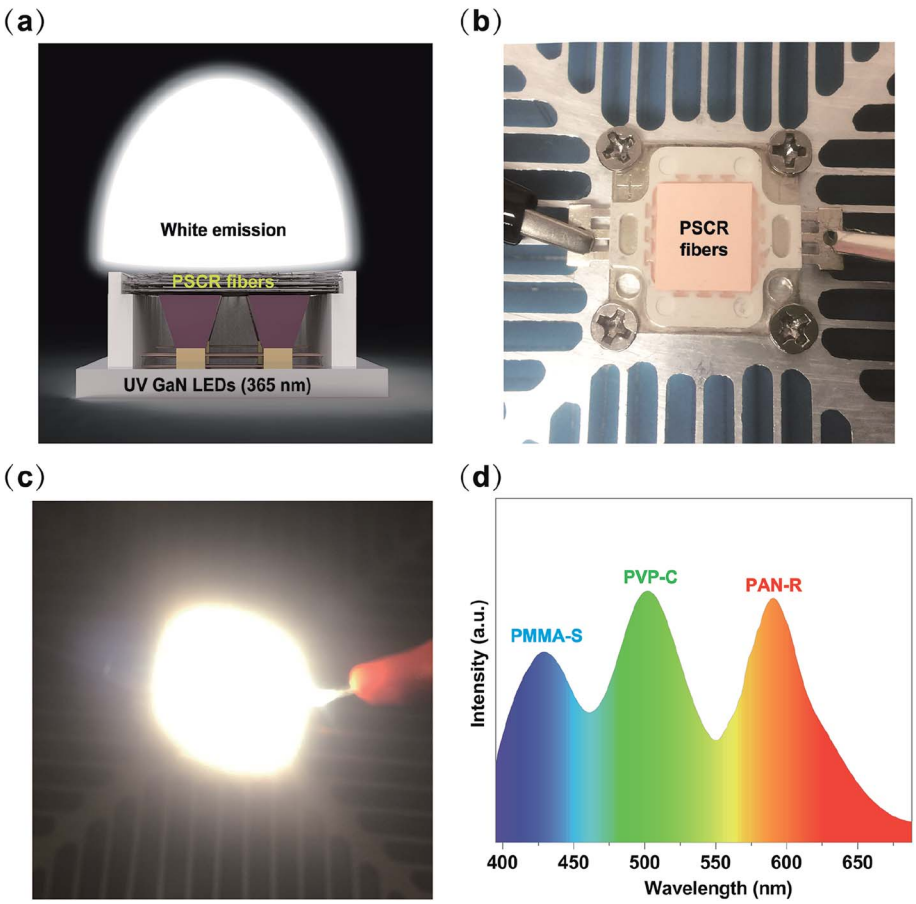

Fig. 7 Diagram (a) and photographs (b) of the configuration of the prototype LED device combining UV LED chips with a PSCR membrane. (c) WLED operated at an applied voltage of 9 V. (d) The electroluminescence spectrum of a PSCR membrane LED.

(Fig. 6b). The above results indicated that PSCR membranes exhibited light stability to some extent, because the dyes remain in their respective isolated areas without diffusion. Moreover, to investigate the UV-Vis absorption of the polymer matrix, we fabricated a PMMA/PVP/PAN fibrous membrane without fluorescent dyes. Fig. S6† shows the UV-Vis absorption spectrum of the PMMA/PVP/PAN membrane. The result presented an absorption peak at around 216 nm and slight absorption in the range of visible light wavelengths. It is indicated that the polymer matrix has little influence on the luminescence performance of the PSCR membrane.

Furthermore, in order to demonstrate the possibility of employing a PSCR membrane as a white emitting layer in LEDs, we assembled a rough WLED by combining a PSCR membrane and a UV LED chip (365 nm) by a remote packaging method (Fig. 7a and b). The resultant WLED exhibits bright white light at an applied voltage of 9 V (Fig. 7c). Fig. 7d demonstrates the electroluminescence spectrum of the PSCR LED. The PSCR membrane was pumped by the LED below to collect effective white light emission through the down conversion process. Therefore, the white light emitting PSCR membrane has potential applications in lighting and display backlighting.

4. Conclusions

In summary, we have demonstrated the production of white-light-emitting PSCR fibrous membranes *via* a triphasic electrospinning approach. The three fluorescent dyes in the fibers can be separated and isolated by a triphasic electrospinning spinneret, thereby limiting the FRET between them, and a wider emission spectrum is obtained in the visible spectrum range (from 382 to 700 nm). Furthermore, the PSCR fibrous membrane was applied to a LED as a light conversion layer by remote packaging, and bright white light was obtained. With superior optical properties and flexibility, the PSCR fibrous membranes exhibit potential for lighting and backlight display devices.

Conflicts of interest

There are no conflicts to declare.

Acknowledgements

The authors acknowledge the National Research Foundation of Korea (NRF) grant funded by the Korea government (MSIT) (2019R1A5A8080326), and the program for fostering next-generation researchers in engineering of the National Research Foundation of Korea (NRF) funded by the Ministry of Science, ICT (No. 2017H1D8A2030449) for financial support.

References

1 J. h. Cho, J. H. Park, J. K. Kim and F. F. Schubert, *Laser Photonics Rev.*, 2017, **11**, 1600147.
2 X. Dai, Y. Deng, X. Peng and Y. Jin, *Adv. Mater.*, 2017, **29**, 1607022.
3 H. Zhao, J. Ni, J. J. Zhang, S. Q. Liu, Y. J. Sun, H. Zhou, Y. Q. Li and C. Y. Duan, *Chem. Sci.*, 2018, **9**, 2918.
4 P. Malakar, D. Modak and E. Prasad, *Chem. Commun.*, 2016, **52**, 4309.
5 Q. Dai, M. E. Foley, C. J. Breshike, A. Lita and G. F. Strouse, *J. Am. Chem. Soc.*, 2011, **133**, 15475.
6 J. Luo, X. Li, Q. Hou, J. B. Peng, W. Yang and Y. Cao, *Adv. Mater.*, 2007, **19**, 1113.
7 S. Huo, P. Duan, T. Jiao, Q. Peng and M. Liu, *Angew. Chem., Int. Ed.*, 2017, **56**, 12174.
8 M. D. Smith and H. I. Karunadasa, *Acc. Chem. Res.*, 2018, **51**, 619.
9 H. Shao, X. Bai, H. Cui, G. Pan, P. Jing, S. Qu, J. Zhu, Y. Zhai, B. Dong and H. Song, *Nanoscale*, 2018, **10**, 1023.
10 F. Schütt, M. Zapf, S. Signetti, J. Strobel, H. Krüger, R. Röder, J. Carstensen, N. Wolff, J. Marx, T. Carey, M. Schweichel, M. I. Terasa, L. Siebert, H. K. Hong, S. Kaps, B. Fiedler, Y. K. Mishra, Z. Lee, N. M. Pugno, L. Kienle, A. C. Ferrari, F. Torrisi, C. Ronning and R. Adelung, *Nat. Commun.*, 2020, **11**, 1437.
11 G. Haider, M. Usman, T. Chen, P. Perumal, K. Lu and Y. Chen, *ACS Nano*, 2016, **10**, 8366.
12 M. F. Budyka, K. F. Sadykova and T. N. Gavrishova, *J. Photochem. Photobiol., A*, 2012, **241**, 38.
13 V. B. Bojinov, A. I. Venkova and N. I. Georgiev, *Sens. Actuators, B*, 2009, **143**, 42.
14 N. Hendler, B. Belgorodsky, E. D. Mentovich, M. Gozin and S. Richter, *Adv. Mater.*, 2011, **23**, 4261.
15 J. Gotta, T. B. Shalom, S. Aslanoglou, A. Cifuentes Rius, N. H. Voelcker, R. Elnathan, O. Shoseyov and S. Richter, *Adv. Funct. Mater.*, 2018, **28**, 1706967.
16 Y. Chen, X. Mao, H. Shan, J. Yang, H. Wang, S. Chen, F. Tian, J. Yu and B. Ding, *RSC Adv.*, 2014, **4**, 2756.
17 P. Grandgeorge, N. Krins, A. Hourlier Fargette, C. Laberty Robert, S. Neukirch and A. Antkowiak, *Science*, 2018, **360**, 296.
18 X. Wang, Z. Huang, D. Miao, J. Zhao, J. Yu and B. Ding, *ACS Nano*, 2018, **13**, 1060.
19 H. J. Kim, J. H. Kim, K. W. Jun, J. H. Kim, W. C. Seung, O. H. Kwon, J. Y. Park, S. W. Kim and I. K. Oh, *Adv. Energy Mater.*, 2016, **6**, 1502329.
20 S. K. Sami, S. Siddiqui, S. Shrivastava, N. Lee and C. Chung, *Small*, 2017, **13**, 1702142.
21 F. Guo, H. You, D. Zhang and S. Chen, *Org. Electron.*, 2018, **63**, 52.
22 Y. Hu, L. Chen, H. Jung, Y. Zeng, S. Lee, K. M. K. Swamy, X. Zhou, M. H. Kim and J. Yoon, *ACS Appl. Mater. Interfaces*, 2016, **8**, 22246.
23 N. Kaerkitcha and T. Sagawa, *Photochem. Photobiol. Sci.*, 2018, **17**, 342.
24 A. Camposeo, F. Di Benedetto, R. Stabile, A. A. R. Neves, R. Cingolani and D. Pisignano, *Small*, 2009, **5**, 562.
25 F. Gu, H. Yu, P. Wang, Z. Yang and L. Tong, *ACS Nano*, 2010, **4**, 5332.
26 L. Zhao, S. Xie, X. Song, J. Wei, Z. Zhang and X. Li, *Biosens. Bioelectron.*, 2017, **91**, 217.

27 Z. Qin, P. Zhang, Z. Wu, M. Yin, Y. Geng and K. Pan, *Mater. Des.*, 2018, **147**, 175.
28 J. D. Starr and J. S. Andrew, *J. Mater. Chem. C*, 2013, **1**, 2529.
29 M. Pan, W. M. Liao, S. Y. Yin, S. S. Sun and C. Y. Su, *Chem. Rev.*, 2018, **118**, 8889.
30 J. Cornelio, T. Y. Zhou, A. Alkaş and S. G. Telfer, *J. Am. Chem. Soc.*, 2018, **140**, 15470.
31 K. C. Tang, M. J. Chang, T. Y. Lin, H. A. Pan, T. C. Fang, K. Y. Chen, W. Y. Hung, Y. H. Hsu and P. T. Chou, *J. Am. Chem. Soc.*, 2011, **133**, 17738.
32 G. Hu, Y. Sun, J. Zhuang, X. Zhang, H. Zhang, M. Zheng, Y. Xiao, Y. Liang, H. Dong, H. Hu, B. Lei, C. Hu and Y. Liu, *Small*, 2019, **16**, 1905266.
33 Z. Z. Li, F. Liang, M. P. Zhuo, Y. L. Shi, X. D. Wang and L. S. Liao, *Small*, 2017, **13**, 1604110.
34 A. Kazemi and J. Lahann, *Small*, 2008, **4**, 1756.
35 M. Yoshida, K. H. Roh and J. Lahann, *Biomaterials*, 2007, **28**, 2446.
36 M. Huang, R. Yu, K. Xu, S. Ye, S. Kuang, X. Zhu and Y. Wan, *Chem. Sci.*, 2016, **7**, 4485.
37 J. H. Wu, W. C. Chen and G. S. Liou, *Polym. Chem.*, 2016, **7**, 1569.
38 A. Reisch and A. S. Klymchenko, *Small*, 2016, **12**, 1968.
39 B. Andreiuk, A. Reisch, E. Bernhardt and A. S. Klymchenko, *Chem.–Asian J.*, 2019, **14**, 836.
40 M. S. Strozyk, D. J. de Aberasturi, J. V. Gregory, M. Brust, J. Lahann and L. M. Liz Marzán, *Adv. Funct. Mater.*, 2017, **27**, 1701626.
41 V. Vohra, G. Calzaferri, S. Destri, M. Pasini, W. Porzio and C. Botta, *ACS Nano*, 2010, **4**, 1409.